Proton-proton bremsstrahlung: Coulomb effect*

Leon Heller and Marvin Rich
Los Alamos Scientific Laboratory, University of California, Los Alamos, New Mexico 87544
(Received 31 August 1973; revised manuscript received 1 May 1974)

A nonrelativistic potential model calculation of proton-proton bremsstrahlung is carried out in which the Coulomb potential as well as double scattering are treated exactly. The conventional electromagnetic current operator for point protons with charge and magnetic moment is used. Cross sections differential with respect to the photon angle are calculated in the symmetric, coplanar Harvard geometry for proton angles of 10, 20, and 30°, at laboratory energies of 5, 20, 42, 62, 99, and 158 MeV, using the Hamada-Johnston potential. Cross sections integrated over the photon angle are presented over a wider range of angles. Including the Coulomb potential lowers the cross section by amounts which are comparable with the errors of the most accurate experiments, and at proton angles smaller than any of the existing experiments the Coulomb effect becomes quite large. Cross sections for the asymmetric Orsay experiment are also computed, including the effect of noncoplanarity, and there is a large discrepancy at some of the experimental points.

[NUCLEAR REACTIONS $p(p,p\gamma)$; calculated $\sigma(\theta_\gamma)$ for lab proton energies 5 to 158 MeV, including Coulomb effects.]

I. INTRODUCTION

Nucleon-nucleon bremsstrahlung has been proposed[1] as a method for choosing between different potentials which fit the elastic scattering data equally well. (The reason one wants a potential is the great simplification it provides for calculations of nuclear properties and reactions.) Bremsstrahlung appears comparatively clean as it involves only a single pair of nucleons and a photon, whose interaction with the nucleons can be treated to lowest order. If the electromagnetic Hamiltonian is taken as the conventional nonrelativistic sum of terms due to the charges and (total) magnetic moments of two point protons, then one is faced with a straightforward but lengthy computational program as outlined in Ref. 1. A nucleon-nucleon potential is assumed, the Schrödinger equation is solved for the initial and final strongly interacting scattering wave functions, and then the bremsstrahlung matrix element is calculated by treating the electromagnetic interaction to first order. This is repeated for other potentials and their bremsstrahlung predictions are compared with experiment, thereby picking out the best potential. This program has been carried out to some extent but there are complications both of a fundamental and a practical nature.

There are at least two reasons why the electromagnetic interaction described above cannot be exact. The first is that the charge and current densities which have been used, $\rho_1(\vec{x})$ and $\vec{j}_1(\vec{x})$, do not form the components of a four-vector under Lorentz transformations. This is a consequence of the fact that they were obtained from the total energy operator and the *nonrelativistic* kinetic energy operator in the Schrödinger equation by making the "minimal" replacement $i\partial/\partial t \to i\partial/\partial t - \sum_j e_j A^0(\vec{r}_j)$, and $-i\vec{\nabla}_j \to -i\nabla_j - e_j\vec{A}(\vec{r}_j)$. A^0 and $\vec{A}$ are the time and space components of the vector potential. The charge and current densities can be identified from the electromagnetic interaction generated in this way, and they are just the familiar expressions

$$\langle\psi_f|\rho_1(\vec{x})|\psi_i\rangle = e_1\int d^3r_2\psi_f^*(\vec{x},\vec{r}_2)\psi_i(\vec{x},\vec{r}_2) + e_2\int d^3r_1\psi_f^*(\vec{r}_1,\vec{x})\psi_i(\vec{r}_1,\vec{x}),$$

$$\langle\psi_f|\vec{j}_1(\vec{x})|\psi_i\rangle = \frac{e_1}{2m_1 i}\int d^3r_2\psi_f^*(\vec{x},\vec{r}_2)\vec{\nabla}_x\psi_i(\vec{x},\vec{r}_2) + \frac{e_2}{2m_2 i}\int d^3r_1\psi_f^*(\vec{r}_1,\vec{x})\vec{\nabla}_x\psi_i(\vec{r}_1,\vec{x}) \tag{1}$$

$$+\mu_1\mathrm{curl}_x\int d^3r_2\psi_f^*(\vec{x},\vec{r}_2)\vec{\sigma}_1\psi_i(\vec{x},\vec{r}_2) + \mu_2\mathrm{curl}_x\int d^3r_1\psi_f^*(\vec{r}_1,\vec{x})\vec{\sigma}_2\psi_i(\vec{r}_1,\vec{x}).$$

e_i, m_i, and μ_i are the charge, mass, and total magnetic moment of the ith particle, and $\rho\vec{\nabla}\chi \equiv \rho\vec{\nabla}\chi - \chi\vec{\nabla}\rho$. The terms involving the magnetic moments which have been included are the standard nonrelativistic expressions. The wave functions are understood to contain Pauli spinors for the two particles.

While relativistic corrections to the magnetic moment terms in Eq. (1) have been written down and included in some bremsstrahlung calculations,[2] there is no clear cut procedure for correcting the terms involving the charge. This is due to the fact that the next term in the expansion of $[M^2 - (\vec{\nabla} - ie\vec{A})^2]^{1/2}$, namely $(\vec{\nabla} - ie\vec{A})^4/8M^3$, completely changes the character of the Schrödinger equation from second order to fourth order.[3] Although the effect of including the terms involving $(\vec{A}\cdot\vec{\nabla})\nabla^2/M^3$ has been found[4] to be less than 1.5% at 200 MeV, the uncertainty as to the correct procedure to be followed does not encourage us to try to apply relativistic corrections to the current in Eq. (1) at any significantly higher energy. In particular, if bremsstrahlung experiments are to be performed at meson factory energies, we would want to start from some dynamical theory which is covariant.

It should be mentioned that there does exist a calculation which is fully relativistic,[5] but in which the strong interaction is treated only to lowest order. No further consideration of relativistic questions will be given in the present paper.

A second shortcoming of the electromagnetic current in Eq. (1) is that it is not conserved if the potential in the Schrödinger equation has any nonlocality.[6] Since all realistic potentials describing the nucleon-nucleon system do have nonlocal terms, corrections for their presence have to be made. This will be considered further in a future paper where the extent of the ambiguity in the corrections is examined.

The calculations which are reported in this paper use the current given in Eq. (1), with wave functions found by solving the Schrödinger equation with the Hamada-Johnston (HJ) potential.[7] Comparisons with the results from another potential will be given in a future paper. It was natural to divide up the work this way because the second potential—which produces exactly the same elastic scattering as the HJ potential—has considerably more nonlocality than the HJ potential, and requires more consideration of how the electromagnetic current should be modified.

The primary difference between the present paper and previous bremsstrahlung calculations is that we include the Coulomb potential along with the HJ potential when calculating the wave functions. Approximate treatments of the Coulomb effect by other authors will be discussed at the end of Sec. III. For small proton angles the effect of including the Coulomb potential becomes very dramatic and this will be shown in the graphs. We also include the double scattering term, which so far has been calculated only by Brown.[8]

Details of the method of calculation are given in Sec. II. The Coulomb effect is discussed in Sec. III, and the results are shown in Sec. IV. Lengthy equations have been relegated to an Appendix at the end of this paper. We use units in which $\hbar = c = 1$.

II. CALCULATION OF THE BREMSSTRAHLUNG CROSS SECTION

Labeling all particles by their momenta, we are considering the process

$$p_1 + p_2 \rightarrow p_1' + p_2' + k\,.$$

The Hamiltonian is

$$H = H_0^N + H_0^{EM} + V + H', \tag{2}$$

where H_0^N is the sum of the kinetic energies of the two nucleons and H_0^{EM} is the free Hamiltonian for the electromagnetic field. V is the (strong) interaction between the two nucleons and H' describes the interaction between the nucleons and the electromagnetic field. This last term contains a small coupling constant and will be treated to first order. The bremsstrahlung matrix element is written

$$T = (E_1E_2E_1'E_2'k)^{1/2}\langle\psi_f^{(-)}; k, \epsilon|H'|\psi_i^{(+)}\rangle\,, \tag{3}$$

where $|k, \epsilon\rangle$ is an eigenstate of H_0^{EM} describing a photon of momentum k and polarization ϵ. The E_i and E_i' are the initial and final total energies of the nucleons. The state $|\psi_i^{(+)}\rangle$ is a solution of the Schrödinger equation

$$(H_0^N + V)|\psi\rangle = i\,\frac{\partial}{\partial t}\,|\psi\rangle \tag{4}$$

which contains a plane wave of unit amplitude with the asymptotic momenta, plus an outgoing scattered wave. $|\psi_f^{(-)}\rangle$ is written similarly with an incoming scattered wave. H' can be written in terms of the charge and current densities $\rho(\vec{x})$ and $\vec{j}(\vec{x})$ as

$$H' = \int d^3x[A^0(\vec{x})\rho(\vec{x}) - \vec{A}(\vec{x})\cdot\vec{j}(\vec{x})] \tag{5}$$

and taking the part of the matrix element in Eq. (3) which refers to the photon gives

$$T = (E_1E_2E_1'E_2')^{1/2}\left(\frac{2\pi}{k}\right)^{1/2} \times\int d^3x e^{-i\vec{k}\cdot\vec{x}}\langle\psi_f^{(-)}|\epsilon^0\rho(\vec{x}) - \vec{\epsilon}\cdot\vec{j}(\vec{x})|\psi_i^{(+)}\rangle\,. \tag{6}$$

In this paper the charge and current densities are taken to be $\rho_1(\vec{x})$ and $\vec{j}_1(\vec{x})$ defined in Eq. (1). The limitations of this procedure have already been touched upon in the Introduction, and will not be taken up again until a future paper. We work in a gauge with $\epsilon^0 = 0$ and $\vec{\epsilon}\cdot\vec{k} = 0$. Writing each wave function as the product of a plane wave for the center of mass coordinate with total momentum $\vec{P}_{i,f}$ times a function of the relative coordinate $\psi_{i,f}(\vec{r})$, and carrying out the integration over $\vec{x}$ in Eq. (6) gives, for equal mass particles

$$T = -(2\pi)^3\delta^{(3)}(\vec{P}_i - \vec{P}_f - \vec{k})\vec{\epsilon}\cdot\vec{M},$$

$$\vec{M} \equiv (E_1E_2E_1'E_2'k)^{1/2}\left(\frac{2\pi}{k}\right)^{1/2}\int d^3r\left\{\frac{1}{2mi}(e_1e^{-i\vec{k}\cdot\vec{r}/2} - e_2e^{i\vec{k}\cdot\vec{r}/2})[\psi_f^*(\vec{r})\vec{\nabla}_r\psi_i(\vec{r})]\right.$$
$$\left. + i\,\psi_f^*(\vec{r})(e^{-i\vec{k}\cdot\vec{r}/2}\mu_1\vec{k}x\vec{\sigma}_1 + e^{i\vec{k}\cdot\vec{r}/2}\mu_2\vec{k}x\vec{\sigma}_2)\psi_i(\vec{r})\right\}. \tag{7}$$

In writing Eq. (7) we have dropped a term proportional to $(\vec{P}_i + \vec{P}_f)$ by evaluating $\vec{M}$ in the center of mass system in which this vector is in the direction $\vec{k}$, and making use of the transversality condition. Specializing to two protons with $\mu = 2.792e/2m$, and again using the transversality condition leads to the final expression

$$\vec{M} = (E_1E_2E_1'E_2'k)^{1/2}\left(\frac{2\pi}{k}\right)^{1/2}\frac{e}{m}\int d^3r\left\{-2\sin\frac{\vec{k}\cdot\vec{r}}{2}\,\psi_f^*(\vec{r})\vec{\nabla}_r\psi_i(\vec{r})\right.$$
$$\left. + \frac{\kappa}{2}\,\psi_f^*(\vec{r})\left[i\cos\frac{\vec{k}\cdot\vec{r}}{2}\vec{k}x(\vec{\sigma}_1 + \vec{\sigma}_2) + \sin\frac{\vec{k}\cdot\vec{r}}{2}\vec{k}x(\vec{\sigma}_1 - \vec{\sigma}_2)\right]\psi_i(\vec{r})\right\}, \tag{8}$$

where $\kappa = 2.792$.

The differential cross section for unpolarized initial particles, summed over the polarizations of all the final particles is

$$d\sigma = \frac{1}{2}\frac{1}{4}\sum_{s,m}\sum_{s',m'}\frac{2\pi}{B}(\vec{M}^*\cdot\vec{M} - |\vec{M}\cdot\vec{k}/k|^2)\rho, \tag{9}$$

where the invariant flux B and the invariant density of states ρ are expressed in terms of laboratory variables as $B = m|\vec{p}_1|$:

$$\rho = \frac{1}{(2\pi)^6}\frac{1}{E_1'}\frac{p_2'^3p_1'^2(\partial p_1'/\partial\theta_\gamma)}{|p_2'^2(E_2' + k) + E_2'\vec{p}_2'\cdot(\vec{p}_1' - \vec{p}_1)|}\,d\theta_\gamma d\Omega_1 d\Omega_2. \tag{10}$$

The summations in Eq. (9) are over the initial and final total spins (of the protons) and components along the beam axis. The solid angles in Eq. (10) refer to the two protons, and θ_γ is the polar angle of the photon.

The initial and final wave functions must be antisymmetrized in the spin and space coordinates. Writing the spatial parts of the initial and final relative wave functions at infinity as $\exp(i\vec{p}_{i,f}\cdot\vec{r})$ $\pm\exp(-i\vec{p}_{i,f}\cdot\vec{r})$, the factor of $\frac{1}{2}$ in Eq. (9) corrects for the normalization of the initial state.

III. TREATMENT OF THE COULOMB POTENTIAL

In high angular momentum states where the nuclear potential is unimportant, the proton-proton wave function becomes a Coulomb function, φ^c, so we write $\psi = \varphi^c + (\psi - \varphi^c)$ for both the initial and final states, and the matrix element becomes a sum of four terms

$$\langle\psi_f|H_{em}|\psi_i\rangle = \langle\varphi_f^c|H_{em}|\varphi_i^c\rangle + \langle\varphi_f^c|H_{em}|\psi_i - \varphi_i^c\rangle$$
$$+ \langle\psi_f - \varphi_f^c|H_{em}|\varphi_i^c\rangle$$
$$+ \langle\psi_f - \varphi_f^c|H_{em}|\psi_i - \varphi_i^c\rangle, \tag{11}$$

where

$$H_{em} \equiv \int d^3x\,\vec{\epsilon}\cdot\vec{j}(\vec{x})\exp(-i\vec{k}\cdot\vec{x}).$$

The first term is pure Coulomb bremsstrahlung, the second and third terms are called single nuclear scattering, and the last term is double nuclear scattering. The pure Coulomb bremsstrahlung matrix element can be evaluated analytically,[9] and is very small over the entire range of energies and angles reported on, of the order of a few nb/sr^2. One could attempt to evaluate the single scat-

tering terms in analogy to their treatment in the absence of the Coulomb potential: first write $\psi - \varphi^c = G^c t^c \varphi^c$ where G^c is the pure Coulomb Green's function and t^c is the nuclear t matrix defined with respect to Coulomb functions—the on-shell values of t^c are measured in elastic scattering—and then insert complete sets of pure Coulomb states into the bremsstrahlung matrix element. In the problem without Coulomb potential this procedure leads to a direct evaluation of each single scattering matrix element as an off-shell t matrix $\times$energy denominator $\times$electromagnetic vertex. With Coulomb functions, however, there would be an integration over the momenta of the complete set of states already in the single scattering terms, and a double integration if the same technique were applied to the double scattering term.

For this reason we decided to evaluate the single and double scattering terms directly in coordinate space. Each ψ in Eq. (8) is expanded in states of definite angular momentum which are obtained by solving the partial wave Schrödinger equation with an assumed nuclear potential plus Coulomb potential. For energies up to 62 MeV we permitted the nuclear potential to act in states of angular momentum up to $j_{max} = 3$, and for higher energies $j_{max} = 5$. Even if $\psi - \phi^c$ vanishes for $j > j_{max}$, there are still single scattering contributions of the form

$$\langle \phi^c_{j>j_{max}} | H_{em} | \psi - \phi^c_{j \le j_{max}} \rangle ,$$

which are limited, however, since $\vec{M}$ receives its dominant contribution from the lowest orbital angular momentum portions of $\cos\frac{1}{2}\vec{k}\cdot\vec{r}$ and $\sin\frac{1}{2}\vec{k}\cdot\vec{r}$, $l = 0$ and 1, respectively. (For energies up to 62 MeV we retained just these l values which correspond to magnetic dipole radiation plus portions of the electric dipole and electric quadrupole. Above 62 MeV we kept $l = 2$ and 3, which extends through magnetic octupole and portions of the electric octupole and electric hexadecapole.) At 158 MeV we included states in ϕ^c through $j = 9$ (which is the maximum value that can be connected to $j = 5$ with $l = 1$) and we have verified that all terms higher than $l = 3$ or $j = 9$ make negligible contributions to the matrix element. Table I illustrates this at $\theta = 10°$, $\theta_\gamma = 40°$. At 99 MeV we omitted the states from $j = 6$ to 9; they contribute less than 3% to the cross section.

After the angular integration in Eq. (8) is carried out [for just the final three terms in Eq. (11); the first term is done analytically] there remain radial integrals of the form

$$\int_0^\infty u_f(r)\, j_l(\tfrac{1}{2}kr) u_i(r) dr ,$$

where each u is either a Coulomb function or the difference of an exact wave function and a Coulomb function, for definite angular momentum. There are two additional integrals arising from the term in Eq. (8) with the gradient operator; these involve du/dr or an extra factor of r^{-1}. All these integrals were evaluated numerically up to a large radius R, and analytically beyond. Although the u's become linear combinations of regular and irregular Coulomb functions once the nuclear potential becomes negligible, we were not able to end the numerical integration there, simply be-

TABLE I. Breakdown of the contributions to the p-p bremsstrahlung cross section at 158 MeV, $\theta = 10°$, $\theta_\gamma = 40°$ by angular momenta for the Coulomb function ϕ^c, and also for the photon, according to Eqs. (8)–(11). Since the nuclear potential only acted in states up to $j_{max} = 5$, the double scattering term terminates there. The first column, $j = 0$–5, includes single and double scattering, and shows the *changes* in the cross section due to the addition of more angular momenta for the photon. The second column shows the changes in the cross section due to four additional angular momenta in the Coulomb functions. All contributions underlined were included in the 158 MeV results presented in this paper.

$\sin\{\frac{1}{2}\vec{k}\cdot\vec{r}\}$ / $\cos\{\frac{1}{2}\vec{k}\cdot\vec{r}\}$ \ ϕ^c	Single scattering $j = 0$–5	$j = 6$–9	$j > 9$
$l = 0, 1$	<u>0.347</u>	<u>−0.025</u>	0
$l = 2, 3$	<u>−0.013</u>	<u>0.001</u>	
$l = 4, 5$	−0.001		

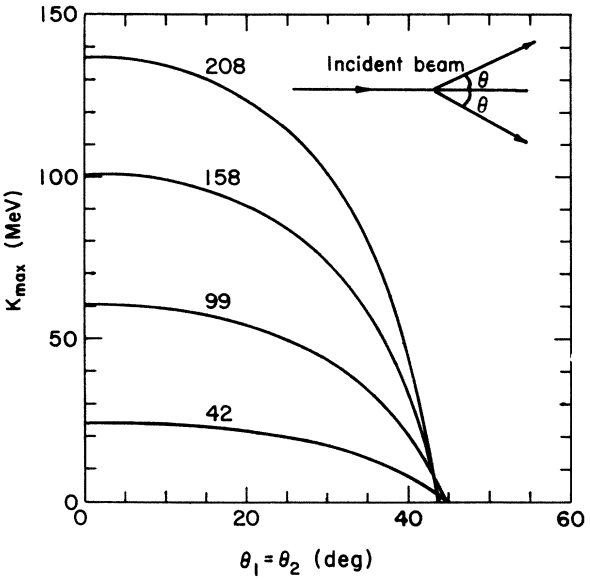

FIG. 1. The maximum possible photon energy as a function of the (common) angle of the two protons in the coplanar symmetric geometry. The maximum occurs when the photon goes forward. Curves are labeled by the incident proton energy (in MeV). The insert in the upper right corner illustrates the geometry.

cause we did not have a general analytic expression for the indefinite integral of a product of Coulomb (and Bessel) functions (and a power of r). As a result we were forced to continue the numerical integration out to much larger distances where the asymptotic series for the Coulomb functions becomes valid. A value of R approximately equal to 200 fm was adopted. Tests of this procedure on known integrals of the same general type gave excellent agreement with the exact answers.

Marker and Signell[10] have carried out an approximate evaluation of the Coulomb effect on nucleon-nucleon bremsstrahlung. Their starting point is the conventional one in which all the Coulomb functions in Eq. (11) are replaced by plane waves (it is still a correct identity), and then the scattered wave is expressed in terms of the free particle Green's function, $\psi - \varphi = G_0 t \varphi$, where t is the t matrix due to the sum of the nuclear and Coulomb potentials, $t = \langle \varphi \mid V_N + V_c \mid \psi^{(+)} \rangle$. $\psi^{(+)}$ is the exact solution with both nuclear and Coulomb potentials present. Marker and Signell make two approximations to evaluate t. (i) In the term $\langle \varphi \mid V_N \mid \psi^{(+)} \rangle$ they replace $\psi^{(+)}$ by the solution of the problem in which the Coulomb potential is absent; this should be a good approximation if the energy is not too small. (ii) The term $\langle \varphi \mid V_c \mid \psi^{(+)} \rangle$ (which they call the Coulomb correction) is approximated by the *on-shell pure Coulomb scattering amplitude* at some energy intermediate between the initial and final values. Since $\psi^{(+)}$ has strong nuclear distortion in the low angular momentum states we find it very surprising that this procedure gives a good result. We judge that to be the case by comparing the cross sections integrated over photon angle in Ref. 10, with and without Coulomb correction, to the cross sections calculated by us (and shown in the next section).

As an example of the accuracy of the Marker-Signell procedure, at 62 MeV with the protons at 30° in the Harvard geometry, their approximate treatment of the Coulomb effect lowers the cross section by 0.24 μb/sr^2 (out of a total of 2.7 μb/sr^2). In our exact calculation including the Coulomb effect lowers the cross section by 0.19 μb/sr^2. Considering the uncertainty in the experimental number, ± 0.24 μb/sr^2, their treatment is adequate. For other proton energies at this same angle the conclusion is similar. Since they did not publish

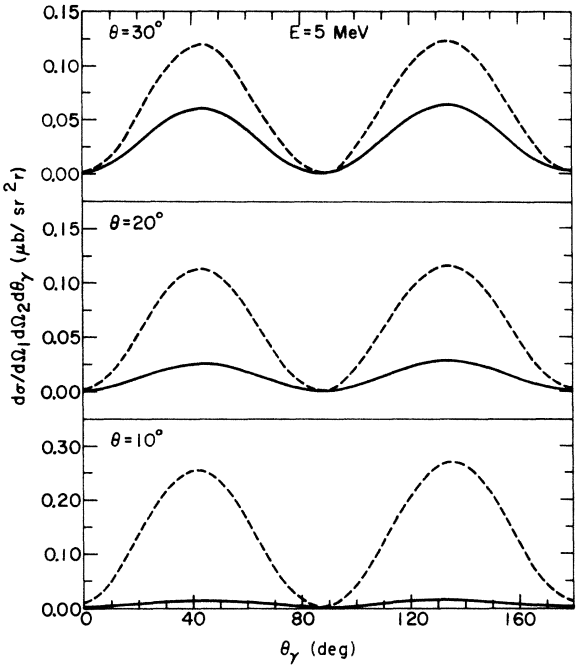

FIG. 2. The differential cross section for proton-proton bremsstrahlung vs photon angle in the symmetric coplanar geometry. The top portion is for protons emerging at 30°; middle portion 20°; and bottom portion 10°. The Hamada-Johnston potential is used, and the solid curve includes Coulomb potential, the dashed curve omits it. Both curves include double scattering. Incident proton energy is 5 MeV.

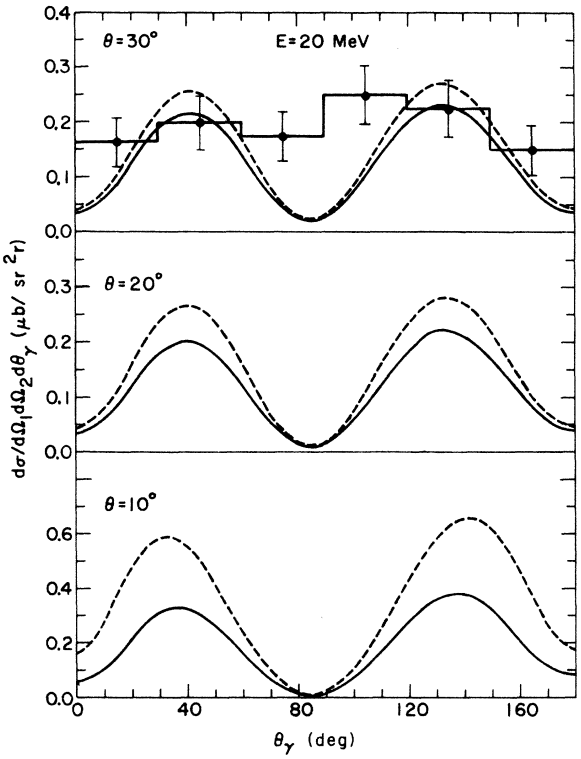

FIG. 3. See caption to Fig. 2. Incident proton energy is 20 MeV. Data are from Ref. 15 and include some effect of noncoplanarity.

results for proton angles less than 25°, where the Coulomb effect becomes larger, we cannot make any comparison there. These small angles, where the p-p system is far off-shell, are the physically interesting ones.

McGuire[11] has performed a calculation at 52 MeV for proton angles of 9°, with a treatment of the Coulomb effect similar to Marker and Signell, but a very different prescription for calculating the t matrix (at this far off-shell point). McGuire found that the Coulomb effect *increases* the cross section by an order of magnitude or more. This is in violent disagreement with our results shown in the next section.

IV. RESULTS

Almost all the calculations reported on in this paper were performed for the symmetric, coplanar, Harvard geometry in which the two protons are detected at equal angles to the beam and making a plane with the beam. Measurement of the energies of both protons overdetermines the event and yields the energy and angle of the photon. Figure 1 shows the maximum possible photon energy as a function of the common polar angle θ of the two protons, for several values of the beam energy. (This maximum occurs when the photon goes forward and the two protons have equal energies.) Since the main reason for performing bremsstrahlung experiments is to learn about the off-shell behavior of the nucleon-nucleon t matrix, one wants to produce photons of the highest possible energy, and this requires proton detectors at the smallest possible angles. Most of the experiments have been performed at $\theta = 30°$, and calculations at this angle are rather insensitive to the choice of potential.[12]

Since the counters often subtend a significant angle out of the plane, it is necessary to calculate the variation of the theoretical cross section with azimuthal angle in order to compare with experimental numbers. Such calculations have been performed by Drechsel and Maximon[13] and we have confirmed their results for a couple of energies. (For the Orsay experiment at 156 MeV, where the proton angles are small and asymmetric, we have performed our own out-of-plane calculations.) Some authors have used the Drechsel and Maximon calculations to extract coplanar cross sections from their data. Marker and Signell[10] tabulated coplanar cross sections $d\sigma/d\Omega_1 d\Omega_2$, integrated over the photon angle, at $\theta = 30$ and 35°, and Hal-

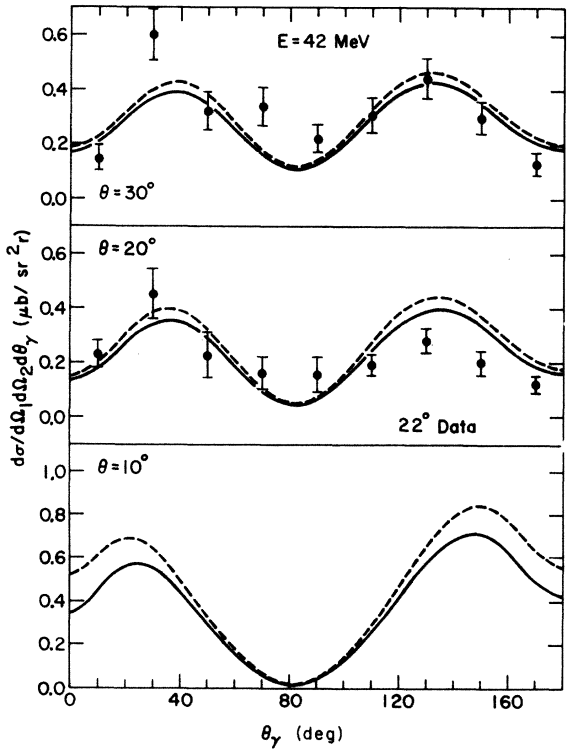

FIG. 4. See caption to Fig. 2. Incident proton energy is 42 MeV. Data are from J. V. Jovanovich *et al.* [Phys. Rev. Lett. 26, 277 (1971)] and includes some effect of noncoplanarity.

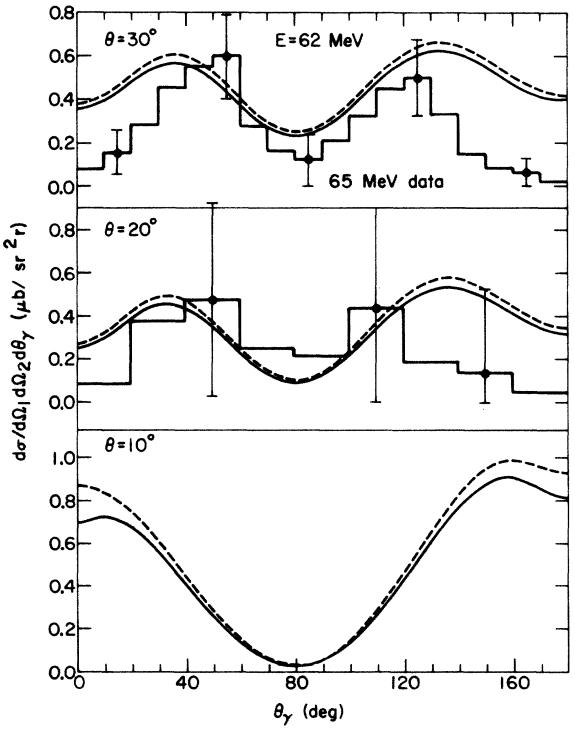

FIG. 5. See caption to Fig. 2. Incident proton energy is 62 MeV. Data are from Ref. 16 and includes some effect of noncoplanarity.

bert[14] has brought this up to date with all the data available as of 1971, including nonsymmetric geometries. We have relied heavily on Halbert's excellent review article, and have indicated with arrows on Fig. 9 those points which he says should be regarded as upper limits rather than true cross sections.

On Figs. 2 to 7 we show photon angular distributions $d\sigma/d\Omega_1 d\Omega_2 d\theta_\gamma$ for proton angles $\theta = 10$, 20, and 30°. The curves are drawn for the coplanar symmetric case. Since the data points which are shown contain noncoplanar contributions as well as the effect of binning, they cannot be directly compared to the curves and are shown just for qualitative purposes. Theoretical histograms which include the effect of noncoplanarity at 20 and 65 MeV are shown in Refs. 15 and 16. The 158 MeV data[17] is nearly coplanar and the required corrections should be very small.

Cross sections integrated over photon angle, $d\sigma/d\Omega_1 d\Omega_2$, are shown on Figs. 8 and 9. As discussed above, these experimental values *have* been corrected for noncoplanarity, and should be compared directly to the calculated curves. There is more data in the symmetric Harvard geometry at other energies and angles,[14] especially large angles, where we have not performed calculations. The agreement between the calculated integrated cross sections and the measured values is fair, with the greatest discrepancy occurring at 99 MeV, 35°. The unusual behavior of this point—which is fairly close to the elastic region and less subject to model dependence—has been noted before.

A look at Figs. 8 and 9 shows that the Coulomb effect is as large as the error bars for a few experimental points. If an experiment were performed near 150 MeV at angles less than 10°—which would be very interesting for learning about the potential—the Coulomb effect would be quite important.

The figures also show the effect of omitting the double scattering term (with no Coulomb potential). This decreases the cross section for proton angles of 30° and increases it for 10°, with the largest effect occurring when the photon is nearly forward

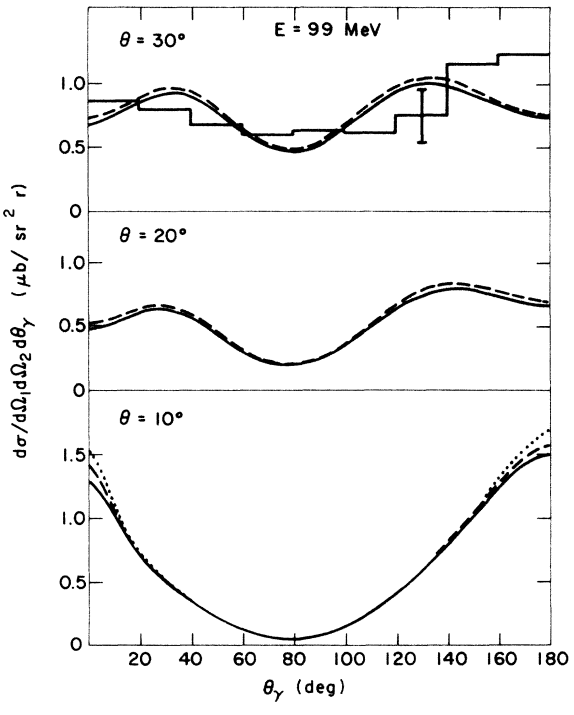

FIG. 6. See caption to Fig. 2. The dotted curves omit double scattering as well as the Coulomb potential. Incident proton energy is 99 MeV. Data are from F. Sannes, J. Trischuk, and D. G. Stairs [Nucl. Phys. A146, 438 (1970)] and includes some effect of noncoplanarity.

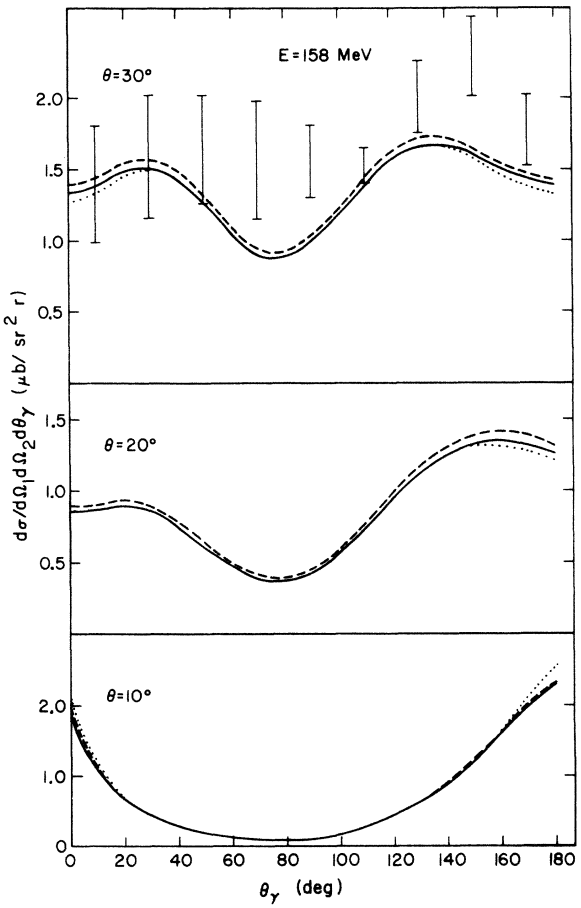

FIG. 7. See caption to Fig. 2. The dotted curves omit double scattering as well as the Coulomb potential. Incident proton energy is 158 MeV. Data are from Ref. 17.

or backward, At 158 MeV, 30°, our result for the size of the double scattering term is in good agreement with Brown's[18] over the whole photon angular distribution. Although this is the only published result for double scattering in the symmetric geometry, we are also in excellent agreement with an unpublished[19] result at $E = 158$ MeV, 10°, $\theta_\gamma = 2.6°$, where the omission of double scattering increases the cross section by 0.29 $\mu b/sr^2 r$.

The agreement for the actual magnitude of the cross section at this energy is not quite as good. Table II shows a comparison of our calculations without Coulomb potential at 158 MeV, 20°, with those in Ref. 8, taken from Fig. 11 of that paper. We do not understand the discrepancy at backward photon angles. At 62 MeV, on the other hand, we agree very well with Brown's cross sections.

A recent experiment performed at Orsay[20] at

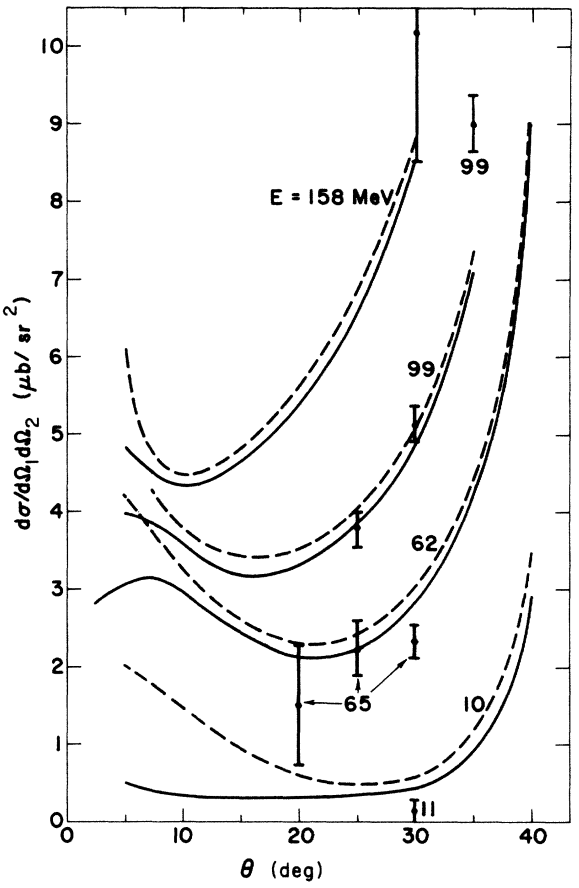

FIG. 8. Cross section for proton-proton bremsstrahlung integrated over the angular distribution of the photon vs the proton angle in the symmetric coplanar geometry. Curves are labeled with the energy of the incident proton. The Hamada-Johnston potential is used, and the solid curves include the Coulomb potential, dashed curves omit it. Data are from these references: 11 MeV: W. Wölfle and R. Müller, Jahresbericht 1970, Laboratorium für Kernphysik, Eidgenössische Technische Hochschule, Zurich (unpublished), p. 26; A. M. Green, private communication; 65 MeV: Ref. 16; 99 MeV: F. Sannes, J. Trischuk, and D. G. Stairs, Phys. Rev. Lett. 21, 1474 (1968); Nucl. Phys. A146, 438 (1970); 158 MeV: Ref. 17.

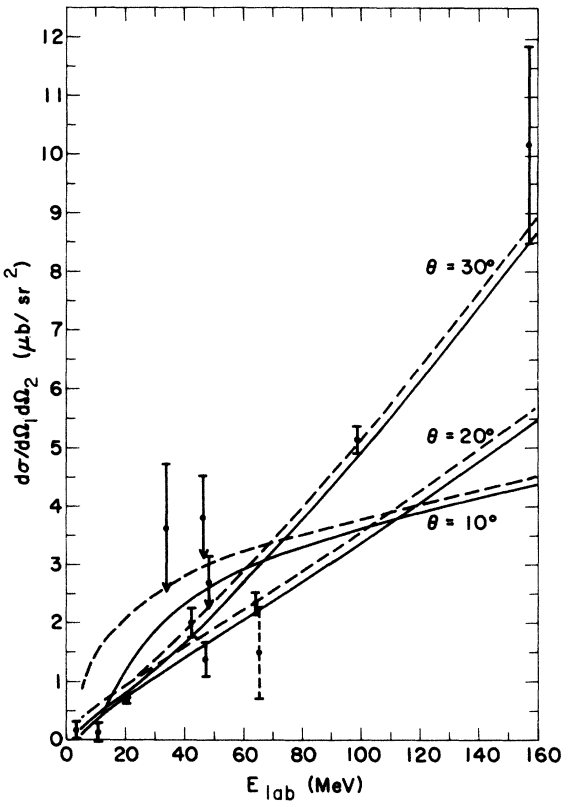

FIG. 9. Cross section for proton-proton bremsstrahlung integrated over the angular distribution of the photon vs the energy of the incident proton in the symmetric coplanar geometry. Curves are labeled with the angle of the emerging protons. The Hamada-Johnston potential is used, and the solid curves include the Coulomb potential, dashed curves omit it. All the data are at 30° except for the one point marked 20°. The data at 11, 65, 99, and 158 MeV are from the references given in the caption to Fig. 8. Other data are from these references: 3.5 MeV: E. A. Silverstein and K. G. Kibler, Phys. Rev. Lett. 21, 922 (1968); 33.5 and 46 MeV: I. Slaus *et al.*, Phys. Rev. Lett. 17, 536 (1966); 42 MeV: J. V. Jovanovich *et al.*, Phys. Rev. Lett. 26, 277 (1971); 47.1 MeV: D. L. Mason, M. L. Halbert, and L. C. Northcliffe, Phys. Rev. 176, 1159 (1968); 48 MeV: R. E. Warner, Can. J. Phys. 44, 1225 (1966); 64.4 MeV: D. O. Galde, M. L. Halbert, C. A. Ludemann, and A. van der Woude, Phys. Rev. Lett. 25, 1581 (1970); 65.0 MeV: Ref. 16. The points with arrows on them are to be considered as upper limits, according to Ref. 14, which should be consulted for other comments about the data.

TABLE II. Comparison of our cross sections for symmetric coplanar p-p bremsstrahlung at 158 MeV, 20°, with those calculated by Brown (Ref. 19). All numbers are computed with the Hamada-Johnston potential and without the Coulomb potential. Units are $\mu b/sr^2 r$.

θ_γ (deg)	Brown $j \leq 4$	Present work $j \leq 5$
30	0.90	0.89
60	0.50	0.50
120	1.08	0.98
150	1.48	1.38

156 MeV detects one proton at $\theta_1 = 15°$ and the other at $\theta_2 = 18$, 21, 24, or 27° (on the other side of the beam). This is a region which is somewhat sensitive to the potential.[12] To reduce background, the photon was also detected in a range of angles in the back hemisphere on the same side of the beam as the 15° detector. Brown[21] found agreement with the data at the (15°, 18°) point, but the calculations and experiment diverge as θ_2 increases.

Since the detectors subtend a significant angle out of the plane, we have computed noncoplanar cross sections to see how this modified Brown's results. A word of caution is in order. In Ref. 20 it is stated that "no corrections were needed for noncoplanarity"; and also that "the maximum noncoplanar angle φ (in the notation of Drechsel and Maximon) was 9.6°...." If this latter statement were correct, there would be a large correction for noncoplanarity. [Indeed, with the exception of the (15°, 18°) point, a portion of the proton detectors would have been beyond the kinematically allowed region. This is due to the fact that the photon detector reaches back to approximately 150°, and the farther backward (or forward) the photon goes, the more nearly the coplanar is the event constrained to be.] We have since learned[22] that the number 9.6° refers to *two times* the variable φ defined by Drechsel and Maximon,[13] $\varphi \equiv \frac{1}{2}(180° + \varphi_2 - \varphi_1)$. As θ_2 decreases from 27 to 18°, φ_{exp} increases[22] from 4.8 to 5.7°. (These values are in reasonable agreement with what one calculates from the statement in Ref. 20 that the proton detectors subtend an angle at the target of ±1.5° in the vertical plane.)

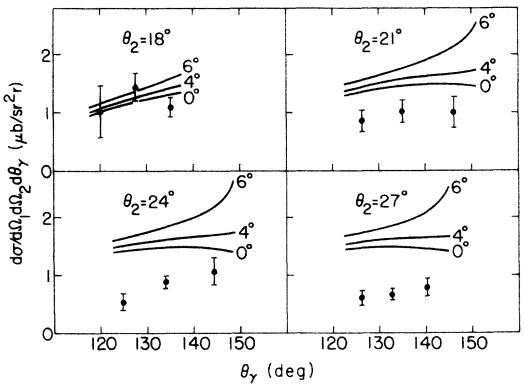

FIG. 10. Differential cross sections for the 156 MeV Orsay experiment, Refs. 20 and 22. Proton number 1 is detected at 15° to the beam, and proton number 2 at the four different angles shown. The curves are computed with the Hamada-Johnston plus Coulomb potentials, for three different values of the out-of-plane variable $\varphi \equiv \frac{1}{2}(180° + \varphi_2 - \varphi_1)$: $\varphi = 0°$ (coplanar), 4°, and 6°. The maximum experimental value of φ is 4.8° at $\theta_2 = 27°$, and increases to 5.7° at $\theta_2 = 18°$.

Lacking detailed information about the efficiency of the detectors as a function of angle, we simply plot on Fig. 10 the cross sections calculated from the Hamada-Johnston potential at $\varphi = 0°$ (coplanar), 4°, and 6°. Keeping in mind the fact that—as a result of parity conservation and analyticity—the cross section vs φ is flat at $\varphi = 0$, the coplanar value will be emphasized when an actual integration over the detectors is carried out. Examination of Fig. 10 shows qualitatively that the effect of noncoplanarity is to make the discrepancy between theory and experiment somewhat *greater* than it was though to be when the coplanar calculations were made.[21] The calculations shown on Fig. 10 include the Coulomb potential. Omitting it raises the cross sections by almost 5%.

If the true normalization were such as to *raise* the data by the full uncertainty[20] of ±12%, this would reduce the discrepancy with the calculations, but it would still be several standard deviations at $\theta_2 = 24$ and 27°. Before concluding that the Hamada-Johnston potential is unable to fit this data, which would be an extremely interesting result, it is important to consider what corrections need to be applied to the calculations. The ones which pertain to the electromagnetic current will be taken up in a second paper, but we would be surprised if they shift the calculations by as much as 1 standard deviation of the data.

Relativistic corrections have been calculated by Celenza *et al.*[23] for the conditions of this experiment and they find[24] that these lower the coplanar calculations at $\theta_2 = 27°$ by ~5% at the small θ_γ end of the detector, and ~12% at the large θ_γ end. This reduces the discrepancy but still leaves it large. For example, at $\theta_2 = 27°$, $\theta_\gamma = 126.2°$, the theory is off by 5 standard deviations. Even if the experimental value is raised by 12% corresponding to the normalization uncertainty, the discrepancy is still more than 4 standard deviations.

V. SUMMARY

The Coulomb effect in proton-proton bremsstrahlung calculations is not negligible for some of the existing experiments, and will be quite important if experiments are performed at very small proton angles.

If the large discrepancy between theory and experiment at 156 MeV persists when all corrections are included, the Hamada-Johnston potential will be ruled out. It will be interesting to see if *any* potential can fit these data along with the elastic scattering data.

ACKNOWLEDGMENTS

We would like to thank Dr. P. Signell for many discussions about bremsstrahlung and for giving us some unpublished cross sections. Dr. V. R. Brown kindly provided some unpublished cross sections which helped us to locate an error in our calculation. We wish to thank Dr. B. F. Gibson and Dr. M. K. Liou for informing us of the size of the relativistic corrections for the Orsay experiment in advance of publication; and correspondence with Dr. N. Marty helped to clarify the size of the noncoplanarity effect. We thank M. Menzel for performing the calculations for Fig. 1.

APPENDIX

In this Appendix, we have compiled the principal equations used in the calculation of proton-proton bremsstrahlung discussed above. These equations have been separated into three groups: the first relating to the calculation of the proton-proton scattering wave functions, the second displaying the partial wave expansions of the four amplitudes which specify the bremsstrahlung process, and the third giving the expression for the bremsstrahlung cross section in terms of these amplitudes. Some of these relations may be found in other articles or texts, but are repeated here for the sake of completeness and explicitness.

A. Proton-proton scattering equations

The partial wave expansions for the singlet even and triplet odd two-proton wave functions used in the present calculation are, respectively,

$$\psi_0(\vec{p},\vec{r}) = \frac{8\pi}{pr} \sum_{\substack{l \\ \text{even}}} \sum_{m=-l}^{l} i^l e^{i(\phi_l + \delta_l^0)} u_l(pr) Y_{l,m}(\hat{r}) Y_{l,m}^*(\hat{p}) \chi_0 \tag{A1}$$

and

$$\psi_{1,m_s}(\vec{p},\vec{r}) = \frac{8\pi}{pr} \sum_{j=0}^{\infty} \sum_{\substack{l=|j-1| \\ \text{odd}}}^{j+1} \sum_{m=-l}^{l} \sum_{\substack{l'=|j-1| \\ \text{odd}}}^{j+1} \sum_{\substack{l''=|j-1| \\ \text{odd}}}^{j+1} \sum_{\mu=-1}^{1} i^l (Q_{ll}^{-1}{}_{l''} e^{i\phi_{l''}})$$

$$\times \begin{pmatrix} l & 1 \\ m & m_s \end{pmatrix} \begin{vmatrix} j \\ m+m_s \end{pmatrix} \begin{pmatrix} l' & 1 \\ m+m_s-\mu & \mu \end{vmatrix} \begin{matrix} j \\ m+m_s \end{matrix} \Big) \chi_{1,\mu} Y_{l',m+m_s-\mu}(\hat{r}) Y_{l,m}^*(\hat{p}) w_{l'',l'}^j(p,r). \tag{A2}$$

Here, $\vec{p}$ is the relative momentum of the two protons in their center of mass system, m_s is the z component of the triplet spin, ϕ_l and δ_l^0 are the pure Coulomb and singlet even phase shifts for scattering in angular momentum state l, and χ_0 and $\chi_{1,\mu}$ are the singlet spin function and the triplet spin function with z projection of μ, Clebsch-Gordan coefficients for the coupling of angular momenta l_1 and l_2 to angular momentum j are represented by

$$\begin{pmatrix} l_1 & l_2 \\ m_1 & m_2 \end{vmatrix} \begin{matrix} j \\ m \end{matrix} \Big).$$

A factor of $1/\sqrt{2}$, related to the antisymmetrization, has been omitted from these functions.

The singlet even functions $u_l(pr)$ and the triplet odd functions $w_{1,1}^0(pr)$ and $w_{l,l}^l(pr)$ satisfy the uncoupled wave equation

$$\left(\frac{d^2}{dr^2} - \frac{l(l+1)}{r^2} - \frac{me^2}{\hbar^2 r} + p^2\right) f_l^{js}(r) - \frac{m}{\hbar^2} V_{l,l}^{js} f_l^{js}(p,r) = 0, \tag{A3}$$

where m is the proton mass, $V_{l,l}^{js}(r)$ is the appropriate nuclear potential, and index $s = 0, 1$ distinguishes singlet from triplet states. The remaining triplet functions are solutions of the coupled equations

$$\left(\frac{d^2}{dr^2} - \frac{l''(l''+2)}{r^2} - \frac{me^2}{\hbar^2 r} + p^2\right) w_{l,l''}^j(p,r) - \frac{m}{\hbar^2} V_l^{j1}{}_{,l''}(r) w_{l,l''}^j(p,r) - \frac{m}{\hbar^2} V_l^{j1}{}_{l''+2,l''}(r) w_{l,l''+2}^j(p,r) = 0,$$

$$\left(\frac{d^2}{dr^2} - \frac{(l''+2)(l''+3)}{r^2} - \frac{me^2}{\hbar^2 r} + p^2\right) w_{l,l''+2}^j(p,r) - \frac{m}{\hbar^2} V_l^{j1}{}_{,l''+2}(r) w_{l,l''}^j(p,r) - \frac{m}{\hbar^2} V_l^{j1}{}_{l''+2,l''+2}(r) w_{l,l''+2}^j(p,r) = 0. \tag{A4}$$

The index l of functions $w^j_{l,l''}(pr)$ labels the two distinct pairs of solutions obtained from Eqs. (A4). Solutions of Eq. (A3) are normalized to the asymptotic form

$$f^{js}_l(r) \sim \cos\delta^s_l \sin(\lambda_l + \phi_l) + \sin\delta^s_l \cos(\lambda_l + \phi_l),$$

where

$$\lambda_l = pr - \eta \ln 2\, pr - \frac{l\pi}{2}$$

and η is given by the Breit relativistic prescription[25]

$$\eta = \frac{e^2}{\hbar v_{\text{lab}}} = e^2 \Big/ \left\{ \hbar c \left[1 - \left(\frac{(mc^2)^2}{(mc^2)^2 + 2(\hbar c p)^2} \right)^2 \right]^{1/2} \right\}.$$

If the asymptotic form of the solutions of Eqs. (A4) are written as

$$w^j_{l,l''}(pr) \sim C_{l,l''} \sin(\lambda_{l''} + \phi_{l''}) + D_{l,l''} \cos(\lambda_{l''} + \phi_{l''})$$

and

$$w^j_{l,l''+2}(pr) \sim C_{l,l''+2} \sin(\lambda_{l''+2} + \phi_{l''+2}) + D_{l,l''+2} \cos(\lambda_{l''+2} + \phi_{l''+2}),$$

proper normalization is achieved in Eq. (A2) by taking $Q^{-1}_{l,l''}$ to be

$$Q^{-1}_{l,l''} = e^{i\phi_l} (C - iD)^{-1}_{l,l''} e^{-i\phi_{l''}}.$$

For the uncoupled triplet states of Eq. (A2)

$$Q^{-1}_{l,l''} = \delta_{l,l''} e^{i\delta^1_l}.$$

B. Partial wave expansion of the bremsstrahlung transition amplitudes

The $pp\gamma$ transition amplitude in the center of mass system has been given by Eq. (8). In order to carry out the spatial integrations indicated there, partial wave expansions of the initial and final two-proton state functions and of the emitted photon state have been used. The expansions for the proton wave functions have already been given by Eqs. (A1) and (A2) above. For the photon functions, we have used

$$\sin\frac{\vec{k}\cdot\vec{r}}{2} = 4\pi \sum_{\substack{L \\ \text{odd}}} \sum_{M=-L}^{L} i^{L-1} j_L\left(\frac{kr}{2}\right) Y_{L,M}(\hat{k}) Y^*_{L,M}(\hat{r}) \tag{A5a}$$

and

$$\cos\frac{\vec{k}\cdot\vec{r}}{2} = 4\pi \sum_{\substack{L \\ \text{even}}} \sum_{M=-L}^{L} i^{L} j_L\left(\frac{kr}{2}\right) Y_{L,M}(\hat{k}) Y^*_{L,M}(\hat{r}) \tag{A5b}$$

rather than a more complicated multipole expansion. Four distinct amplitudes are listed, depending on whether the initial and final protons are in a singlet or triplet state. Insertion of the various partial wave expansions into the amplitude integral

$$-\vec{M} \propto \vec{T}_{fi} = \int d^3r \psi^*_f(\vec{r}) \left[2 \sin\frac{\vec{k}\cdot\vec{r}}{2} \nabla_r + \frac{\kappa}{2} \left(i \cos\frac{\vec{k}\cdot\vec{r}}{2} (\vec{\sigma}_1 + \vec{\sigma}_2)\vec{k} + \sin\frac{\vec{k}\cdot\vec{r}}{2} (\vec{\sigma}_1 - \vec{\sigma}_2)\vec{k} \right) \right] \psi_i(\vec{r}) \tag{A6}$$

gives the following expressions upon performance of the angular integrations:
(1) Singlet to singlet

$$\vec{T}_{0,0} = \frac{8(4\pi)^2}{pp'} \sum_{s=-1}^{1} \vec{e}^*_s \sum_{\substack{l \\ \text{even}}} \sum_{m=-l}^{l} \sum_{\substack{L \\ \text{odd}}} \sum_{M=-L}^{L} \sum_{\substack{l_1 \\ \text{even}}} \sum_{J=|l_1-1|}^{l_1+1}$$

$$\times (2l_1+1) \left(\frac{2l+1}{2L+1} \right)^{1/2} j^{3l+l_1+L-1} e^{i(\phi_l + \delta_l)} e^{i(\phi_{l_1} + \delta_{l_1})} Y^*_{l,m}(\hat{p}') Y_{L,M}(\hat{k}) \begin{pmatrix} l_1 & 1 & J \\ 0 & 0 & 0 \end{pmatrix} \begin{pmatrix} l_1 & 1 & J \\ 0 & s & s \end{pmatrix} \begin{pmatrix} l & J & L \\ 0 & 0 & 0 \end{pmatrix} \begin{pmatrix} l & J & L \\ m & s & M \end{pmatrix}$$

$$\times \int_0^\infty dr\, u_l(p'r) j_L\left(\frac{kr}{2}\right) \left(\frac{d u_{l_1}(pr)}{dr} + \frac{(l_1 - J)(l_1 + J + 1)}{2} \frac{u_{l_1}(pr)}{r} \right); \tag{A7}$$

(2) singlet to triplet

$$\vec{T}_{1,0}(m_f)=\frac{\kappa}{2}\frac{8(4\pi)^2}{pp'}\sum_{s=-1}^{1}\vec{e}_s^{\,*}\times\vec{k}\sum_{j=0}^{\infty}\sum_{\substack{l=|j-1|\\ \text{odd}}}^{j+1}\sum_{m=-l}^{l}\sum_{\substack{l'=|j-1|\\ \text{odd}}}^{j+1}\sum_{\substack{l''=|j-1|\\ \text{odd}}}^{j+1}\sum_{L}$$

$$\times\sum_{M=-L}^{L}\sum_{\substack{l_1\\ \text{even}}}(2l_1+1)\left(\frac{2l'+1}{2L+1}\right)^{1/2}i^{3l+l_1+L-1}(Q_{l,l''}{}^{-1}e^{i\phi_{l''}})e^{i(\phi_{l_1}+\delta_{l_1})}Y^*_{l,m}(\hat{p}')Y_{L,M}(\hat{k})$$

$$\times\begin{pmatrix} l & 1 & \\ m & m_f & m+m_f\end{pmatrix}\begin{pmatrix} l' & 1 & \\ m+m_f-s & s & m+m_f\end{pmatrix}\begin{pmatrix} l' & l_1 & \\ 0 & 0 & 0\end{pmatrix}\begin{pmatrix} l' & l_1 & \\ m+m_f-s & 0 & M\end{pmatrix}$$

$$\times\int_0^\infty dr\,w^{j}_{l'',l'}(p'r)j_L\left(\frac{kr}{2}\right)u_{l_1}(pr);\tag{A8}$$

(3) triplet to singlet

$$\vec{T}_{0,1}(m_i)=\frac{\kappa}{2}\frac{8(4\pi)^2}{pp'}\sum_{s=-1}^{1}\vec{e}_s\times\vec{k}\sum_{\substack{l\\ \text{even}}}\sum_{m=-l}^{l}\sum_{\substack{L\\ \text{odd}}}\sum_{M=-L}^{L}\sum_{j_1=0}^{\infty}\sum_{\substack{l_1=|j_1-1|\\ \text{odd}}}^{j_1+1}$$

$$\times\sum_{\substack{l_1'=|j_1-1|\\ \text{odd}}}^{j_1+1}\sum_{\substack{l_1''=|j_1-1|\\ \text{odd}}}^{j_1+1}\left(\frac{(2l+1)(2l_1+1)(2l_1'+1)}{2L+1}\right)^{1/2}i^{3l+l_1+L-1}e^{i(\phi_l+\delta_l)}(Q_{l_1,l_1''}{}^{-1}e^{i\phi_{l_1''}})Y^*_{l,m}(\hat{p}')Y_{L,M}(\hat{k})$$

$$\times\begin{pmatrix} l & l_1' & \\ 0 & 0 & 0\end{pmatrix}\begin{pmatrix} l & l' & \\ m & m_i-s & M\end{pmatrix}\begin{pmatrix} l_1 & 1 & \\ 0 & m_i & m_i\end{pmatrix}\begin{pmatrix} l_1' & 1 & \\ m_i-s & s & m_i\end{pmatrix}$$

$$\times\int_0^\infty dr\,u_l(p'r)j_L\left(\frac{kr}{2}\right)w^{j_1}_{l_1'',l_1'}(pr);\tag{A9}$$

(4) triplet to triplet

$$\vec{T}_{1,1}(m_f,m_i)=\vec{R}_{1,1}(m_f,m_i)+i\frac{\kappa}{2}\vec{S}_{1,1}(m_f,m_i),\tag{A10}$$

where the gradient interaction gives

$$\vec{R}_{1,1}(m_f,m_i)=\frac{8(4\pi)^2}{pp'}\sum_{\lambda=-1}^{1}\vec{e}_\lambda^{\,*}\sum_{j=0}^{\infty}\sum_{\substack{l=|j-1|\\ \text{odd}}}^{j+1}\sum_{m=-l}^{l}\sum_{\substack{l'=|j-1|\\ \text{odd}}}^{j+1}\sum_{\substack{l''=|j-1|\\ \text{odd}}}^{j+1}\sum_{\substack{L\\ \text{odd}}}$$

$$\times\sum_{M=-L}^{L}\sum_{j_1=0}^{\infty}\sum_{\substack{l_1=|j_1-1|\\ \text{odd}}}^{j_1+1}\sum_{\substack{l_1'=|j_1-1|\\ \text{odd}}}^{j_1+1}\sum_{\substack{l_1''=|j_1-1|\\ \text{odd}}}^{j_1+1}\sum_{J=|l_1'-1|}^{l_1'+1}\sum_{s=-1}^{1}$$

$$\times\left(\frac{(2l'+1)(2l_1+1)(2l_1'+1)}{(2L+1)}\right)^{1/2}j^{3l+l_1+L-1}(Q_{l,l''}{}^{-1}e^{i\phi_{l''}})(Q_{l_1,l_1''}{}^{-1}e^{i\phi_{l_1''}})Y^*_{l,m}(\hat{p}')Y_{L,M}(\hat{k})$$

$$\times\begin{pmatrix} l & 1 & \\ m & m_f & m+m_f\end{pmatrix}\begin{pmatrix} l' & 1 & \\ m+m_f-s & s & m+m_f\end{pmatrix}\begin{pmatrix} l_1 & 1 & j_1\\ 0 & m_i & m_i\end{pmatrix}$$

$$\times\begin{pmatrix} l_1' & 1 & \\ m_i-s & s & m_i\end{pmatrix}\begin{pmatrix} l_1 & 1 & J\\ 0 & 0 & 0\end{pmatrix}\begin{pmatrix} l_1' & 1 & \\ m_i-s & \lambda & m_i-s+\lambda\end{pmatrix}\begin{pmatrix} l' & J & \\ 0 & 0 & 0\end{pmatrix}\begin{pmatrix} l' & J & \\ m+m_f-s & m_i-s+\lambda & M\end{pmatrix}$$

$$\times\int_0^\infty dr\,w^{j_1}_{l'',l'}(p'r)j_L\left(\frac{kr}{2}\right)\left(\frac{d}{dr}w^{j_1}_{l_1'',l_1'}(pr)+\frac{(l_1'-J)(l_1'+J+1)}{2}\frac{w^{j_1}_{l_1'',l_1'}(pr)}{r}\right)\tag{A11}$$

and the magnetic moment contribution is

$$\vec{S}_{1,1}(m_f,m_i)=\frac{8(4\pi)^2}{pp'}\sum_{s=-1}^{1}\sum_{t=-1}^{1}(-\delta_{s,t+1}\vec{e}_1^{\,*}+\delta_{s,t-1}\vec{e}_{-1}^{\,*}+s\delta_{s,t}\vec{e}_0^{\,*})$$

$$\times\vec{k}\sum_{j=0}^{\infty}\sum_{\substack{l=|j-1|\\ \text{odd}}}^{j+1}\sum_{m=-l}^{l}\sum_{\substack{l'=|j-1|\\ \text{odd}}}^{j+1}\sum_{\substack{l''=|j-1|\\ \text{odd}}}^{j+1}\sum_{\substack{L\\ \text{even}}}\sum_{M=-L}^{L}\sum_{j_1=0}^{\infty}\sum_{\substack{l_1=|j_1-1|\\ \text{odd}}}^{j_1+1}\sum_{\substack{l_1'=|j_1-1|\\ \text{odd}}}^{j_1+1}\sum_{\substack{l_1''=|j_1-1|\\ \text{odd}}}^{j_1+1}$$

$$\times\left(\frac{(2l'+1)(2l_1+1)(2l_1'+1)}{(2L+1)}\right)^{1/2}i^{3l+l_1+L}(Q_{l,l_1''}{}^{-1}e^{i\phi_{l''}})(Q_{l_1,l_1''}{}^{-1}e^{i\phi_{l_1''}})Y_{l,m}^{*}(\hat{p}')Y_{L,M}(\hat{k})$$

$$\times\begin{pmatrix}l & 1\\ m & m_f\end{pmatrix}\begin{vmatrix}j\\ m+m_f\end{vmatrix}\begin{pmatrix}l' & 1\\ m+m_f-s & s\end{pmatrix}\begin{vmatrix}j\\ m+m_f\end{vmatrix}\begin{pmatrix}l_1 & 1\\ 0 & m_i\end{pmatrix}\begin{vmatrix}j_1\\ m_i\end{vmatrix}\begin{pmatrix}l_1' & 1\\ m_i-t & t\end{pmatrix}\begin{vmatrix}j_1\\ m_i\end{vmatrix}\begin{pmatrix}l' & l_1'\\ 0 & 0\end{pmatrix}\begin{vmatrix}L\\ 0\end{vmatrix}$$

$$\times\begin{pmatrix}l' & l_1'\\ m+m_f-s & m_i-t\end{pmatrix}\begin{vmatrix}L\\ M\end{vmatrix}\int_0^{\infty}drw_{l'',l'}^{j}(p'r)j_L\left(\frac{kr}{2}\right)w_{l_1'',l_1'}^{j_1}(pr). \tag{A12}$$

The notation used in the above equations is:

(a) The relative wave vectors of the initial and final proton pairs in their center of mass systems are, respectively, $\vec{p}$ and $\vec{p}'$. The wave vector of the photon is $\vec{k}$.

(b) Unsubscripted l's and j refer to angular momenta of the final state protons, and l_1's and j_1 to the initial state proton angular momenta.

(c) The magnetic quantum of a final proton triplet state is represented by m_f, and that of an initial triplet state by m_i.

(d) $\kappa = 2.792$ is the proton magnetic moment in units of $e\hbar/2mc$.

The radial integrals of these amplitudes were computed as the sum of a numerical integral from $r=0$ to $r=R$ and an analytic integral using asymptotic expansions for the proton wave functions from $r=R$ to $r=\infty$. The separation radius R was chosen so that $u_l(pr)$ and $w_{l'',l'}^{j}(pr)$ could be written in terms of nuclear phase parameters and asymptotic Coulomb functions with a high degree of accuracy.

It should be added that the somewhat forbidding appearance of the above amplitudes due to the large number of summations is, in fact, deceptive.

C. Differential cross section

Taking as independent variables the laboratory polar and azimuthal angles $\Omega \equiv \{\theta, \phi\}$ of each of the two final state protons and the polar angle θ_γ of the outgoing photon, the differential bremsstrahlung cross section for unpolarized initial and final particles may be written as

$$d\sigma/d\Omega_1 d\Omega_2 d\theta_\gamma=\frac{e^2/\hbar c}{(4\pi)^4(mc^2)^3}[E_1E_2E_1'E_2']_{\text{c.m.}}$$

$$\times\left[\sum_{\substack{\text{final}\\ \text{spins}}}\sum_{\substack{\text{initial}\\ \text{spins}}}(\vec{T}^{*}\cdot\vec{T}-|\hat{k}\cdot\vec{T}|^2)\right]_{\text{c.m.}}\frac{p_1^{\,2}p_2^{\,3}}{pE_1[(E+mc^2-E_1)p_1^{\,2}+E_2\vec{p}_2\cdot(\vec{p}_1-\vec{p})]}\frac{\partial(\hbar cp_1)}{\partial\theta_\gamma}. \tag{A13}$$

Brackets subscripted by c.m. indicate that the enclosed quantities are to be calculated in the center of mass system. All other quantities refer to the laboratory frame. Subscripts 1 and 2 refer to the two protons, E_1' and E_2' are their initial energies in the center of mass system, and $\vec{p}$ and E are the wave vector and energy of the incident laboratory proton. Final state quantities are unprimed. The relativistic relation $E=[(\hbar cp)^2+(mc^2)^2]^{1/2}$ is used for all energies. The form $\vec{T}^{*}\cdot\vec{T}-|\hat{k}\cdot\vec{T}|^2$ for the squared transition element follows from the summation over the two polarization states of the photon. Finally, the derivative of the final momentum of proton 1 with respect to the photon angle θ_γ for fixed Ω_1 and Ω_2, which arises from the density of final states factor, is given by the somewhat complicated result of

$$\frac{\partial(\hbar cp_1)}{\partial\theta_\gamma}=\hbar c\,\frac{\alpha D-\gamma}{\delta-\beta D},$$

where

$$\alpha = \sin 2\theta_\gamma \Big\{ p^2 \sin^2\theta_\gamma + p_1^2(\cos^2\theta_1 - \cos^2\theta_\gamma) - 2\vec{p}\cdot\vec{p}_1 \sin^2\theta_\gamma + \left(\frac{mc^2}{\hbar c}\right)^2 \cos^2\theta_\gamma$$
$$+ (\cos^2\theta_2 - \cos^2\theta_\gamma)\left[(\vec{p}-\vec{p}_1)^2 - \left(\frac{mc^2}{\hbar c}\right)^2\right] - A^2 - 2A\cos\theta_2 (p\cos\theta_2 - p_1 \hat{p}_1\cdot\hat{p}_2)\Big\}$$
$$+ 2\sin\theta_\gamma \frac{E + mc^2 - E_1}{\hbar c}[p_1(\cos^2\theta_1 - \cos^2\theta_\gamma) - p\cos\theta_1 \sin^2\theta_\gamma],$$

$$\beta = 2(\cos^2\theta_2 - \cos^2\theta_\gamma)[p_1(\cos^2\theta_1 - \cos^2\theta_\gamma) - p\cos\theta_1\sin^2\theta_\gamma] - 2A\cos\theta_2(\hat{p}_1\cdot\hat{p}_2\cos^2\theta_\gamma - \cos\theta_1\cos\theta_2)$$
$$+ 2\left(\frac{\hbar c p_1}{E_1}\cos\theta_\gamma - \cos\theta_1\right)[A(\cos^2\theta_2 + \cos^2\theta_\gamma) - B\cos\theta_2],$$

$$\gamma = -\left[A^2 + \left(\frac{mc^2}{\hbar c}\right)^2 (\cos^2\theta_2 - \cos^2\theta_\gamma)\right]\Big\{2\sin 2\theta_\gamma (B - A\cos\theta_2)^2 - 4(B - A\cos\theta_2)\Big[\sin 2\theta_\gamma (p\cos\theta_2 - p_1\hat{p}_1\cdot\hat{p}_2)$$
$$- \frac{(E + mc^2 - E_1)}{\hbar c}\cos\theta_2 \sin\theta_\gamma\Big]\Big\} + 2(B - A\cos\theta_2)^2 \cos\theta_\gamma \sin 2\theta_\gamma$$
$$\times\left[\left(\frac{mc^2}{\hbar c}\right)^2 \cos\theta_\gamma + A\frac{(E + mc^2 - E_1)}{\hbar c}\right],$$

$$\delta = 4(B - A\cos\theta_2)\cos^2\theta_\gamma \left[A^2 + \left(\frac{mc^2}{\hbar c}\right)^2 (\cos^2\theta_2 - \cos^2\theta_\gamma)\right]$$
$$\times\left[(\hat{p}_1\cdot\hat{p}_2\cos\theta_\gamma - \cos\theta_1\cos\theta_2) - \cos\theta_2\left(\frac{\hbar c p_1}{E_1}\cos\theta_\gamma - \cos\theta_1\right)\right]$$
$$+ 4A(B - A\cos\theta_2)^2\cos^2\theta_\gamma\left(\frac{\hbar c p_1}{E_1}\cos\theta_\gamma - \cos\theta_1\right),$$

and

$$A = p - p_1\cos\theta_1 - \cos\theta_\gamma \frac{E + mc^2 - E_1}{\hbar c},$$

$$B = p_1(\hat{p}_1\cdot\hat{p}_2\cos^2\theta_\gamma - \cos\theta_1\cos\theta_2) + p\cos\theta_2\sin^2\theta_\gamma,$$

$$D = (\cos^2\theta_2 - \cos^2\theta_\gamma)\left[p^2\sin^2\theta_\gamma + p_1^2(\cos^2\theta_1 - \cos^2\theta_\gamma) - 2pp_1\cos\theta_1\sin^2\theta_\gamma + \left(\frac{mc^2}{\hbar c}\right)^2\cos^2\theta_\gamma\right]$$
$$+ A^2(\cos^2\theta_2 + \cos^2\theta_\gamma) - 2AB\cos\theta_2.$$

---

*Work performed under the auspices of the U. S. Atomic Energy Commission.

[1]M. I. Sobel and A. H. Cromer, Phys. Rev. 132, 2698 (1963).

[2]M. K. Liou and M. I. Sobel, Ann. Phys. (N.Y.) 72, 323 (1972).

[3]One can try to avoid this difficulty by working with the equation satisfied by H^2, where H is the Hamiltonian. This has the appearance of the nonrelativistic Schrödinger equation, but the effective potential is nonlocal if the original potential were local. This creates an uncertainty of order p^2/M^2 in the electromagnetic interaction. We are indebted to Dr. F. Coester for a discussion on this point.

[4]Reference 2 and private communication from Liou and Sobel.

[5]R. Baier, H. Kühnelt, and P. Urban, Nucl. Phys. B11, 675 (1969).

[6]R. H. Thompson and L. Heller, Phys. Rev. C 8, 2355 (1973).

[7]T. Hamada and I. D. Johnston, Nucl. Phys. 34, 382 (1962).

[8]V. R. Brown, Phys. Rev. 177, 1498 (1969) (pp); Phys. Rev. C 6, 1110 (1972) (np).

[9]A. Sommerfeld, *Atombau und Spektrallinien* (Friedr. Vieweg and Sohn, Braunschweig, 1939), Vol. II,

Chap. VII.2; A. Nordsieck, Phys. Rev. 93, 785 (1954).
[10]D. Marker and P. Signell, Phys. Rev. 185, 1286 (1969).
[11]J. H. McGuire, Phys. Lett. 40B, 41 (1972).
[12]L. Heller, Bull. Am. Phys. Soc. 17, 480 (1972).
[13]D. Drechsel and L. C. Maximon, Ann. Phys. (N.Y.) 49, 403 (1968).
[14]M. L. Halbert, in *The Two-Body Force in Nuclei*, edited by S. M. Austin and G. M. Crawley (Plenum, New York, 1972), p. 53.
[15]D. W. Storm and R. Heffner, Phys. Rev. C 4, 1541 (1971).
[16]D. L. Mason, M. L. Halbert, A. van der Woude, and L. C. Northcliffe, Phys. Rev. 179, 940 (1969).
[17]B. Gottschalk, W. J. Shlaer, and K. H. Wang, Nucl. Phys. A94, 491 (1967).
[18]See Fig. 12 of the first paper in Ref. 8.
[19]V. R. Brown, private communication.
[20]A. Willis, V. Comparat, R. Frascaria, N. Marty, M. Morlet, and N. Willis, Phys. Rev. Lett. 28, 1063 (1972); M. Morlet *et al.*, in *Few Particle Problems in the Nuclear Interaction*, edited by I. Slaus *et al.* (North-Holland, Amsterdam, 1972), p. 79. The second of these references contains more recent data.
[21]V. R. Brown, Phys. Rev. C 6, 1110 (1972).
[22]N. Marty, private communication.
[23]L. S. Celenza, M. K. Liou, M. I. Sobel, and B. F. Gibson, Phys. Rev. C 8, 838 (1973). This paper also discusses the effect of noncoplanarity. There are two reasons why the cross sections in this reference are lower than those in Ref. 21 (and therefore closer to the experimental numbers in Ref. 20): One is the relativistic effect; and the other is simply the fact that the calculated *coplanar* cross sections are lower. Part of this is due to the neglect of double scattering.
[24]B. F. Gibson and M. K. Liou, private communication. The relativistic correction increases in magnitude as θ_2 decreases.
[25]G. Breit, Rev. Mod. Phys. 34, 766 (1962).